DMD Fast Forward. Published on July 24, 2008 as doi:10.1124/dmd.108.021493

DMD #21493

Differential Inhibition Of P450s 3A4 and 3A5 By the Newly Synthesized Coumarin Derivatives, 7-Coumarin Propargyl Ether and 7-(4-Trifluoromethyl)coumarin Propargyl Ether

Chitra Sridar, Ute M. Kent, Kate Noon, Alecia Mc Call, Bill Alworth, Maryam Foroozesh and Paul F. Hollenberg

Department of Pharmacology, University of Michigan, Ann Arbor, (C.S., U.M.K., K.N., P.F.H.); Department of Chemistry, Tulane University, New Orleans, LA (B.A.); and Department of Chemistry, Xavier University of Louisiana, New Orleans, LA (A.M.C., M.F.).

Running Title: Differential inhibition of P450 3A4 and 3A5 by coumarin propargyl ethers.

Corresponding Author:

Dr. Paul F Hollenberg, Department of Pharmacology, The University of Michigan, 1150 West Medical Center Dr, Ann Arbor, MI 48109-5632. Phone: (734) 764-8166, Fax: (734) 763-5387, E-mail: phollen@umich.edu

Number of Text Pages: 35

Number of Tables: 3

Number of Figures: 7

Number of References: 34

Number of words in Abstract: 198

Number of words in Introduction: 722

Number of words in Discussion: 1462

Abbreviations: P450, cytochrome P450; CPE, 7-coumarin propargyl ether; TFCPE, 7-(4-trifluoromethyl)coumarin propargyl ether; 7EFC, 7-ethoxy-4-(trifluroromethyl)coumarin; HFC, 7-hydroxy-4-(trifluoromethyl)coumarin; HPLC, high-performance liquid chromatography; LC-MS, liquid-chromatography mass-spectrometry; ESI, electro spray ionization, MS/MS, tandem mass spectrometry; TIC, Total ion chromatogram; XIC, extracted ion chromatogram; THF, tetrahydrofuran.

Abstract.

The abilities of 7-coumarin propargyl ether (CPE) and 7-(4-trifluoromethyl)coumarin propargyl ether (TFCPE) to act as mechanism-based inactivators of P450 3A4 and 3A5 in the reconstituted system have been investigated using 7-benzyloxy-4-(trifluoromethyl)coumarin (BFC) and testosterone as probes. CPE inhibited the BFC *O*-debenzylation activity of P450 3A4 in a time-, concentration-, and NADPH-dependent manner characteristic of a mechanism-based inactivator with a K_I of 112 μM, a k_{inact} of 0.05 min^{-1}, and a $t_{1/2}$ of 13.9 min. Similarly, TFCPE inhibited the BFC *O*-debenzylation activity of P450 3A4 in a time-, concentration-, and NADPH-dependent manner with a K_I of 14 μM, a k_{inact} of 0.04 min^{-1} and a $t_{1/2}$ of 16.5 min. Parallel losses of P450 3A4 enzymatic activity and heme were observed with both compounds as measured by HPLC and reduced-CO spectra. Interestingly, neither compound inhibited the BFC *O*-debenzylation activity of P450 3A5. Reactive intermediates of CPE and TFCPE formed by P450 3A4 were trapped with glutathione and the resulting adducts were identified using tandem mass spectral analysis. Metabolism studies using TFCPE resulted in the identification of a single metabolite that is formed by P450 3A4 but not by P450 3A5 and that may play a role in the mechanism-based inactivation.

The cytochrome P450-dependent mixed function oxidases are the main enzymes involved in the NADPH-dependent metabolism of various xenobiotics to more polar products that can be more readily excreted. In humans, the P450 3A family of enzymes are involved in the metabolism of 50-60% of all currently used drugs (Evans and Relling, 1999). Four major CYP 3A genes have been identified, CYP 3A4, 3A5, 3A7, and 3A43. P450 3A4 is generally thought to be the predominant form expressed in the human liver (Wrighton et al., 2000). P450 3A5 can contribute as much as 50% to the hepatic 3A content in a third of Caucasians and in one half of African Americans (Kuehl et al., 2001). P450 3A7 has been shown to be a fetal form of 3A and little is known about the function of P450 3A43. P450s 3A4 and 3A5 share 84% amino acid sequence homology and thus considerable overlap exists between their substrate specificities (Wrighton and Stevens, 1992). On the other hand, there has also been evidence for preferential metabolism or inactivation of one enzyme over the other. The two enzymes have been shown to exhibit different regio-selectivities toward aflatoxin (Gillam et al., 1995b), increased metabolism of midazolam, tacrolimus and vincristine by P450 3A5 is observed when compared to P450 3A4 (Wandel et al., 1994;Dennison et al., 2006a;Kamdem et al., 2005) and differential inactivation of P450 3A4 and not 3A5 by raloxifene has also been reported (Baer et al., 2007).

Coumarin is a constituent of many plants, microorganisms and animals and is widely used as a fragrance in various products such as cosmetics, soaps, and detergents (Soine T.O, 1964). Coumarins are comprised of an aromatic ring fused to a lactone ring and have been shown to possess a range of pharmacological and biochemical properties. Coumarin has been used in combination therapy with cimetidine in clinical trials for the

treatment of malignant melanomas, metastatic renal carcinomas, and carcinomas of the prostate (Marshall et al., 1989). A number of studies have suggested that coumarin is not toxic to humans, however, species differences exist that could account for variations in both metabolism and toxicity. For example, administration of coumarin to rodents has been shown to produce liver and lung toxicity (Born et al., 1998). Coumarin and coumarin derivatives are known to be substrates for cytochrome P450s (Lake B.G., 1999). Buters et al. used this property to develop a sensitive assay to measure the activities of a number of cytochrome P450s where the *O*-deethylation of 7-ethoxy-(4-trifluoromethyl)coumarin results in the formation of the fluorescent 7-hydroxy-(4-trifluoromethyl)coumarin product (Buters et al., 1993). Thus, coumarin and coumarin derivatives are currently widely used in the drug discovery process.

Many acetylenic compounds have been shown to inactivate various cytochrome P450 enzymes (Strobel et al., 1999;Shimada et al., 1998;Roberts et al., 1997) in a mechanism-based manner that involves binding of a reactive intermediate to either the heme or the apoprotein (Ortiz de Montellano and Kunze, 1980). 2-Ethynylnaphthalene has been shown to inactivate P450s 2B1 and 2B4 through a modification of the apoprotein (Roberts et al., 1994), whereas *tert*-butyl acetylene and *tert*-butyl 1-methyl-2-propynyl ether have been shown to inactivate P450s 2E1 and 2B1, respectively through the formation of both heme- and protein adducts (Blobaum et al., 2002;Von Weymarn et al., 2004).

Naphthoflavones serve as substrates for a number of P450 enzymes (Cho et al., 2003) and the propargyl ether derivatives of naphthoflavones and adamantanes have been shown to be inhibitors of some P450 enzymes. The purpose of this project was to evaluate

compounds that combine both the structural motif of P450 3A substrates with a functional group that has been implicated in the mechanism-based inactivation of P450 enzymes in the hope of finding a compound that will functionally differentiate between P450s 3A4 and 3A5. The development of a unique probe that could differentiate between these two human enzymes would provide a tool to better understand the individual functions of the enzymes in the metabolism of many clinically relevant drugs by human tissues and to investigate the molecular features necessary for substrates and inhibitors to interact with the binding domain of these two closely related enzymes. To that end, 7-coumarin propargyl ether (CPE) and 7-(trifluoromethyl)coumarin propargyl ether (TFCPE) were synthesized (Figure 1) and their effect on the activities of P450s 3A4 and 3A5, as well as their metabolism by these two enzymes, was examined.

.

Materials and Methods

Materials. L-α-dilaurylphosphatidylcholine, L-α-dioleyl-sn-glycero-3-phosphocholine, phosphatidylserine, bovine serum albumin (BSA), NADPH, Tris, catalase, sodium dithionite, and Hepes were purchased from Sigma-Aldrich (St. Louis, MO). 7-Benzyloxy-4-(trifluoromethyl)coumarin (BFC) was obtained from BD Gentest (Woburn, MA). 7-Ethoxy-4-(trifluoromethyl)coumarin (7EFC) was obtained from Molecular Probes (Eugene, OR). AccuBond SPE ODS-C18 cartridges were obtained from Agilent Technologies (Wilmington DE). All other chemicals were of the highest quality commercially available. The human liver microsomes used in the studies have been described previously (Teiber and Hollenberg, 2000)

Purification of Enzymes. P450s 3A4 and 3A5 were expressed in *Escherichia coli* DH5α cells and purified to homogeneity by the method of Gillam et al. (Gillam et al., 1993). P450 NADPH-reductase was expressed in *Escherichia coli* Topp3 cells and purified according to a previously published protocol (Hanna et al., 1998). Cytochrome b5 was purified from liver microsomes of rats (Lin et al., 2002)

Synthesis of coumarin propargyl ethers. The corresponding starting material (0.027 moles of 7-hydroxycoumarin or 7-hydroxy-4-(trifluoromethyl)coumarin purchased from Sigma-Aldrich Chemicals) was dissolved in 30 mL of dry THF under an atmosphere of N_2. Fresh sodium hydride (3 equivalents, 0.081 moles, 1.94 g) was added slowly, followed by 2 equivalents of propargyl bromide (0.054 moles, 6.01 mL). The reaction mixture was left to stir for a week under N_2 and its progress was monitored daily by thin layer chromatography. The reaction was quenched with 50 mL of deionized water and extracted twice with 30 mL portions of methylene chloride. The organic layers were

combined and washed with 10% HCl followed by water (twice). The crude material was then dried over anhydrous $MgSO_4$ and the residual solvent was evaporated under vacuum. The crude product was purified by flash silica gel column chromatography using petroleum ether as the solvent. The pure fractions were combined, and the purified product was re-crystallized from ethanol and water.

CPE. The yield after purification was 90.5%. GC/MS showed >99% purity; *m/z* (%): 200 (19), 51 (100). ^{1}H NMR ($CDCl_3$): δ 2.60 (s, 1H), 4.75 (s, 2H), 6.28 (d, 1H), 6.92 (d, 1H), 6.95 (s, 1H), 7.40 (d, 1H), and 7.65 (d, 1H). ^{13}C NMR ($CDCl_3$): δ 25.60, 56.20, 71.00 102.13, 113.06, 113.18, 113.66, 128.84, 143.29, 155.64, 160.53, and 161.02.

TFCPE. The yield after purification was 25.3%. GC/MS showed >99% purity; *m/z* (%): 268 (1), 202 (100). ^{1}H NMR ($CDCl_3$): δ 2.60 (s, 1H), 4.80 (s, 2H), 6.66 (s, 1H), 6.99 (s, 1H), 7.01 (d, 1H), and 7.65 (d, 1H). ^{13}C NMR ($CDCl_3$): δ 25.60, 56.31, 67.98, 102.71, 107.74, 112.81, 112.87, 113.84, 122.94, 126.46, 156.12, 159.25, and 161.26.

Inactivation assay. The P450s (0.5 nmol) were reconstituted with 1 nmol of reductase, and 0.5 nmol of cytochrome b_5 in the presence of lipid mixture (L-α-dilaurylphosphatidylcholine, L-α-dioleyl-sn-glycero-3-phosphocholine, and phosphatidylserine in a ratio of 1:1:1) and $MgCl_2$ (10 mM). The reconstitution mixture was allowed to sit at room temperature for 20 min and was then diluted to a final volume of 1 ml with 50 mM Hepes (pH7.5), GSH (2 mM), and catalase (250 units). The samples then received either increasing concentrations of 7-(coumarin) propargyl ether in acetonitrile (25 μM to 500 μM, 1 μL/100μL), or 7-(4-trifluoromethyl)coumarin propargyl ether in acetonitrile (5 μM to 100 μM, 1 μL/100μL), or 1 μL/100μL acetonitrile alone in

the control samples. NADPH was added to the samples and 9 pmol each of the P450 in the reconstituted enzyme mixture were transferred at different times to a secondary reaction mixture in a volume of 585 µl containing 1 mM NADPH, 50 µM BFC, 4 mM $MgCl_2$, and 40 µg/mL BSA in 200 mM potassium phosphate buffer (pH 7.4). The reaction mixtures were incubated for 15 min at 37 ºC and then quenched with acetonitrile. The 7-hydroxy product was measured on a Shimadzu RF-5301PC spectrofluorometer (Shimadzu Scientific Instruments, Columbia, MD) with excitation and emission wavelengths of 409 and 530 nm, respectively. The concentration required for half-maximal inactivation (K_I), the maximal rate of inactivation (k_{inact}) and the $t_{½}$ were calculated by linear regression using the Graphpad Prism program (5.0). Inactivation studies using human liver microsomes were performed by incubating two different human liver microsomes (0.3 nmol of each) in the presence of catalase and GSH at the concentrations of CPE and TFCPE indicated above. The reactions were initiated by the addition of NADPH and aliquots were removed to measure activity remaining at 0, 5 and 12 mins as mentioned above.

In addition to BFC, testosterone was used as an alternate substrate probe to test the effect of CPE and TFCPE on P450s 3A4 and 3A5 activity. Reconstitution of the enzymes was carried out as described above. The reaction mixtures were initiated with NADPH and 100 pmol aliquots of the enzyme were transferred at different time points into a secondary assay mixture containing 50 mM Hepes buffer (pH 7.5), 20 mM testosterone, and 1 mM NADPH. The secondary reaction mixtures were incubated for 15 min at 37 ºC and were then terminated by adding 1 mL of ethyl acetate and vortexing. The reaction mixtures were extracted twice and the organic phases were pooled and evaporated under

nitrogen. The dried extracts were suspended in 100 µl of 65% methanol and 75 µL were injected onto a C18 reverse phase column (Microsorb 100 Å, 4.9 × 250 mm; Varian Inc, Walnut Creek, CA) equilibrated with 65% methanol at a flow rate of 1 mL/min. Formation of 6β-hydroxytestosterone was detected after elution from the column under isocratic conditions (65% methanol in water) by its absorbance at 254 nm using a Waters 600E-HPLC coupled to a Waters 501 series pumps, Waters Photodiode Array Detector 996, and a Waters 717 autosampler controlled by Millennium software (Waters, Milford, MA).

Heme analysis. P450 3A4 was reconstituted and inactivated as described above for the activity assays. Samples (100 pmol) of the control and inactivated enzymes were chromatographed on a C4 column (Phenomenex, 250 × 4.6 mm) equilibrated with 30% acetonitrile containing 0.1% TFA. The HPLC system consisted of Waters 501 pumps, a Waters 600E Controller, and a Waters 717A autosampler. The components of the reconstituted mixtures were resolved by linearly increasing the percentage of acetonitrile to 90% over 30 min. Heme was quantified by integrating the area under the peaks that absorbed at 405 nm and mean and standard deviation were calculated from four different experiments. Reduced-CO spectra of the control, exposed, and inactivated samples were obtained by transferring 100 pmol of each sample into 900 µL of quench buffer containing 50 mM potassium phosphate (pH 7.4), 40% glycerol, and 0.6% Tergitol. The samples were bubbled with CO, sodium dithionite was added and the reduced-CO spectra were recorded between 400-500 nm on a DW2 UV/VIS spectrophotometer equipped with an Olis operating system (On Line Instruments Systems, Bogart, GA).

GSH adducts. Samples were reconstituted using 0.5 nmol of P450 3A4 as previously described and incubated in the presence of 10 mM GSH. Reaction conditions and inactivation conditions were the same as described earlier. The reactions were stopped by the addition of 60 µL of 10% TFA/mL of sample and vortexed. The samples were then applied to AccuBond SPE ODS C18 1 mL cartridges. After application of the samples, the cartridges were washed with 2 ml water followed by elution of the GSH-CPE or GSH-TFCPE adducts with 2 ml of methanol followed by 0.3 ml of acetonitrile. The methanol and acetonitrile fractions were combined, dried under nitrogen, and suspended in 50% acetonitrile and 0.5% acetic acid**.** One part of the sample was injected onto a Aqua C18 column (150 mm x 4.6 mm, 5 micron, Phenomenex, Torrance, CA) equilibrated with 5% acetonitrile, 0.1 % acetic acid. The sample components were resolved by eluting at 0.3 mL/min while linearly increasing the percentage of acetonitrile to 90% over the course of 70 min. The LC effluent was directed into a mass spectrometer (LCQ ion trap, ThermoFinnigan) and MS spectra as well as MS/MS spectra were recorded using the data-dependent scanning routine of the Xcalibur data system (ThermoFinnigan). The analyzer conditions were: sheath gas 90 arbitrary units, auxiliary gas 30 arbitrary units, spray voltage 4.5 kV, capillary temperature 170 ºC, capillary voltage 30 V. One full scan between *m/z* 150 -1000 was collected followed by two dependent scans between *m/z* 50 – 1000 at 35% relative collision energy, with an activation Q of 0.250 and an activation time of 30 msec. The second part of the sample was injected into a LC column coupled to a fluorescence detector with excitation at 350 nm and emission at 454 nm. The HPLC system consisted of Shimadzu LC-20AB, autosampler SIL-20AC HT and a Shimadzu fluorescence detector RF-10Axl. The

analysis was carried out using a mobile phase of acetonitrile, 0.1 % acetic acid (phase B) and water, 0.1 % acetic acid (phase A) and a flow rate of 0.3 ml/min. Initial conditions were 5 % B and the percentage of B was maintained for 5 min followed by a linear gradient to 30 % B from 5 to 15 min, to 80 % B from 15 min to 35 min and 90 % B from 35 to 40 min. The column was washed with 90 % B for 15 min before returning to the initial conditions and equilibrating the column for 10 min at the initial conditions before the next injection.

Metabolism of CPE and TFCPE. The formation of 7-OH coumarin was determined to see if P450s 3A4 and 3A5 were able to metabolize the coumarin compounds. This was done by reconstituting P450s 3A4 or 3A5 in presence of CPE or TFCPE as described above. The reactions were allowed to proceed for 30 min after initiating them by the addition of 1mM NADPH. The reaction mixture was then stopped with 70 µl of 15 % TCA. The formation of 7-OH coumarin was analyzed by HPLC using a C18 Microsorb column coupled to a fluorescence detector with excitation at 350 nm and emission at 453 nm. The analysis was carried out using an isocratic mobile phase of 30% methanol with 0.2 % acetic acid. The flow rate was set to 1 ml/ min. Quantitation was done using peak areas by comparing to a standard curve generated with 7-hydroxycoumarin.

LC-APCI-MS and Metabolite analysis. For the metabolism of TFCPE by P450s 3A4 and 3A5 the reconstitution and reaction conditions were as described earlier. The control and the inactivated samples (900 pmol each) were extracted with 2 mL ethyl acetate and the organic phases were dried under nitrogen. The dried samples were resuspended in 100 µl of 50% acetonitrile for chromatographic separation. Chromatographic separation of the metabolites was performed on a Surveyor HPLC system equipped with a quaternary

pump, an autosampler and a diode array detector. The column used was a C18 (either a Microsorb-MV 100°A with a flow rate of 1 mL/min or Phenomenex Jupitor300 5 µm with a flow rate of 0.2 mL/min) reverse-phase column, equilibrated with 90% A and 10% B (A: water, 0.1% acetic acid and B: acetonitrile, 0.1% acetic acid). Metabolites were resolved by increasing the percentage of B as follows: from initial conditions to 30 % over 3 minutes, to 50% B over 5 minutes, holding at 50% B for 2 minutes, increasing to 70% B over 3 minutes, to 90% B over 5 minutes and then holding at 90% B for 2 minutes before returning to initial conditions. A volume of 50µL was injected for each analysis. The elution of the parent compound and the metabolites from the chromatographic column was monitored at 319 nm. Effluent from the HPLC was directed into the atmospheric pressure chemical ionization (APCI) source of a linear ion trap (LTQ, ThermoFinnigan) scanning in the positive ion mode. The ionization source conditions were: APCI vaporizer temperature 450°C, corona discharge voltage 6.0 kV, and tube lens offset voltage of 60 V. Nitrogen was used as the sheath gas (55psi) and auxillary gas (15 psi). Full mass spectra were recorded between m/z 100-2000 and data dependent scanning was used to collect MS/MS spectra of the four most intense ions in each full scan.

Results

Inactivation assay. In the presence of CPE or TFCPE, a time-, concentration-, and NADPH-dependent inactivation of the BFC *O*-debenzylation activity of P450 3A4 in the reconstituted system was observed. Pseudo first-order kinetics was observed for concentrations of CPE between 25 and 500 μM (Figure 2) and for concentrations of TFCPE between 5 to 100 μM (Figure 3). As calculated from the data in Figure 2, the concentration required for half-maximal inactivation (K_I) by CPE was 112 μM, the rate of inactivation (k_{inact}) was 0.05 min^{-1}, and the $t_{1/2}$ was 13.9 min (Table 1). The K_I for TFCPE was 14 μM, the k_{inact} was 0.04 min^{-1}, and the $t_{1/2}$ was 16.5 min (Table 1). In contrast to P450 3A4, incubations of P450 3A5 with CPE or TFCPE in the presence of NADPH showed no inactivation of the BFC *O*-debenzylation activity (data not shown). Incubation with either CPE or TFCPE did not result in inactivation of both samples of human liver microsomes (data not shown).

The loss in the 6β-testosterone hydroxylation activity of P450 3A4 when incubated with CPE or TFCPE in a reconstituted system was also investigated and was found to be time-, concentration-, and NADPH dependent. The inactivation was characterized by a K_I of 25 μM, a k_{inact} of 0.014 min^{-1}, and a $t_{1/2}$ of 50 min for CPE and a K_I of 17 μM, a k_{inact} of 0.04 min^{-1}, and a $t_{1/2}$ of 17 min for TFCPE (Table 1).

Heme Analysis. The effects of inactivation by CPE and TFCPE on the amount of P450 3A4 heme remaining were studied by determining the reduced-CO spectra of the inactivated proteins and by determining the amount of heme remaining by comparing the area under the heme peak absorbing at 405 nm from chromatograms of control and the CPE- and TFCPE- inactivated samples resolved by HPLC. The inactivation of P450 3A4

by CPE and TFCPE after a 20 min incubation resulted in approximate losses of 35 and 55% in *O*-debenzylation activity, respectively, as compared to 0 min (Table 2). Some decrease in activity is seen in 0 min samples with the inactivator and with or without the NADPH and also in the samples with inactivators, but - NADPH. Presumably this is due to carryover of the inactivator from the initial reaction mixture to the assay mixture where it can act as a competitive inhibitor. These losses in the activity were accompanied by losses in the ability of the inactivated samples to form reduced-CO spectra. Losses in the levels of the P450 heme as measured by the reduced-CO spectrum were also seen in control samples that were incubated only with inactivator. The reasons for this are not clear. As shown in Table 2, the loss in heme was approximately 30% when compared to the –NADPH control in samples incubated with CPE suggesting that the inactivation was partly due to heme modification. For the inactivation of 3A4 by TFCPE, the loss in activity was approximately 55% when compared to the –NADPH +TFCPE control compared to a 40% loss of heme as measured by HPLC. This suggests that the inactivation could be due partly to heme modification. In each case when the residual heme was measured by HPLC, a small peak eluting at 23.4 min corresponding to a heme adduct was detected in the inactivated samples but not in the control samples (data not shown). LC/MS analysis of the adducted hemes did not reveal the mass of these adducts.

Analysis of GSH adducts. Incubations of P450 3A4 with CPE or TFCPE in the presence of GSH resulted in the formation of CPE- and TFCPE-glutathione adducts (Figs. 4 and 5). Figure 4A shows the total ion chromatogram (TIC) of the CPE-GSH adduct with the primary ion eluting at 22.2 min that was obtained from samples incubated with CPE and GSH in the presence of NADPH. The peak detected by the fluorescence detector eluting

DMD Fast Forward. Published on July 24, 2008 as DOI: 10.1124/dmd.108.021493
This article has not been copyedited and formatted. The final version may differ from this version.

at the same retention time is shown in panel B. The mass spectrum of the peak eluting at 22.2 min is presented in panel C. The MS/MS spectrum of the ion with an m/z of 523.9 shown in panel D exhibited major ions at *m/z* 448.7 $[MH-75]^+$ and 394.7 $[MH-129]^+$ arising from the parent ion at 523.9 by a neutral loss of glycine and pyroglutamate, respectively, which is characteristic of glutathione-conjugated metabolites. The fragment ion at *m/z* at 307.7 is from the protonated GSH moiety arising from the cleavage of the thioester bond. The fragments with *m/z* 319.0 and 291.7 are from the combined loss of glycine and glutamate and glycine, glutamate and CO, respectively. The fragment with *m/z* 216.8 results from the cleavage of the C-S bond between the GSH moiety and the coumarin propargyl ether. The ion at *m/z* 161.8 is most likely obtained from the sum of coumarin and oxygen whereas the ion at *m/z* 178.8 could be from the combined mass of coumarin, oxygen, and a methyl group. The fragmentation pattern for the major ions observed in the MS /MS spectrum of the CPE-GS conjugate is shown in panel E. Figure 5A shows the TIC of the TFCPE adduct with GSH showing a primary ion eluting at 31.31 min. The peak eluting at around 31 min as seen by the fluorescence detector is shown in panel B. The mass spectrum of the peak eluting at 31.3 min is shown in panel C. Panel D shows the MS/MS spectrum of the ion with m/z 591.9. The fragment ion at *m/z* 573.9 is from the loss of water from the TFCPE-GSH molecule. The daughter ions with *m/z* values of 516.9 $[MH-75]^+$, 462.8 $[MH-129]^+$, and 444.8, $[MH-146]^+$ correspond to losses of glycine-, pyroglutamate-, and pyroglutamate and a water molecule, respectively. The ion with *m/z* 426.9 resulted from a subsequent loss of water from the 444.8 ion. The ion with *m/z* 359.8 resulted from the loss of glycine, glutamate, and CO and the 341.8 ion from the further loss of water. The ion with *m/z* 307.6 represents the

DMD Fast Forward. Published on July 24, 2008 as DOI: 10.1124/dmd.108.021493
This article has not been copyedited and formatted. The final version may differ from this version.

mass of GSH and was also seen in the CPE-GSH adduct profiles. The ions with *m/z* 268.8 and 242.5 correspond to the parent $[M+H]^+$ molecule and to a loss of $HC{\equiv}CH$, respectively. The fragmentation pattern for the major ions of the TFCPE-GS adduct observed in the MS/MS spectrum is shown in Fig. 5, panel E.

Metabolism of CPE and TFCPE. The formation of 7-hydroxy coumarin as a result of *O*-deethylation of CPE or TFCPE by 3A4 or 3A5 was measured by reverse-phase HPLC with fluorescence detection. As shown in Table 3, both P450s 3A4 and 3A5 were able to metabolize both of the coumarin propargyl ether compounds to give 7-hydroxy coumarin. The amount of 7-hydroxy coumarin formed by 3A4 in presence of CPE was approximately half of what was seen with TFCPE. With P450 3A5, the amount of 7-hydroxy coumarin formed was approximately the same with both propargyl compounds. Overall, the rate of formation of 7-hydroxy coumarin by P450 3A5 suggests that both coumarin compounds bind as well to 3A5 as to 3A4 and that are readily metabolized by 3A5 even though they do not inactivate it.

LC-APCI-MS and MS/MS analysis of the metabolites of TFCPE by P450 3A4. TFCPE and its metabolites were monitored at 319nm. Panel A in Fig 6 shows the UV trace of the effluent from the HPLC that was directed into the atmospheric pressure chemical ionization. The total ion chromatogram revealed two distinct peaks: the parent peak eluting at 22.78 min and a metabolite of TFCPE eluting at approximately 20.3 min. This metabolite peak was seen only in the samples incubated with P450 3A4 and not in the samples incubated with P450 3A5. The inset shows the MS spectrum of the parent peak eluting at 22.78 min which revealed an intense $[M+ H]^+$ ion with the *m/z* of 269.0 expected for TFCPE. MS/MS analysis of the parent compound generated fragment ions

at *m/z* 240.9 from loss of CO and 213 due to cleavage of the propargyl ether. The fragmentation pattern of the parent peak is shown in Fig 6 panel B. The single metabolite peak eluting at 20.34 min was only observed in 3A4 samples incubated with NADPH and not in control samples (Fig 7, panel A). The mass spectrum of this peak showed ions with *m/z* values at 271.6 and 231.0 as shown in Figure 7, panel A. The fragmentation of the ion with *m/z* 271.6 yielded daughter ions at *m/z* 253.3 from the loss of water, *m/z* 242.99 which occurs from the loss of CO, and at *m/z* 214.33 arising from the loss of C_3H_4 (panel B). We are unable to explain the origin of the ions with the m/z of 197.10 and 161.25. The fragmentation of the ion at *m/z* of 231.0 yielded a daughter ion with a *m/z* 186.95 which is derived from the ring opening of the compound with a subsequent loss of CO_2 (panel E). Currently we are unable to explain the origin of the ion with m/z 166.91. The fragmentation patterns for these metabolites are shown in panels C and E. No similar peak or any other metabolite peak was observed under these conditions for CPE. The incubation of P450 3A5 with TFCPE did not result in any metabolite as seen by LC-APCI-MS suggesting that the product formed by P450 3A4 is unique to this enzyme.

Discussion.

The importance of human P450 3A enzymes arises from their abundant expression and their role in the first-pass metabolism of many clinically important drugs. Until recently, P450 3A4 was thought to be the major human drug metabolizing enzyme. However, it has now been shown that P450 3A5 may represent more than 50% of the total P450 3A content in some individuals (Kuehl et al., 2001). The contribution of P450 3A5 to the metabolic clearance of P450 3A substrates in the liver has not been well characterized. Both P450s 3A4 and 3A5 show similar K_m and V_{max} values for midazolam 1'hydroxylation (Gibbs et al., 1999). Both enzymes metabolize nifedipine (Gillam et al., 1995a), lidocaine (Bargetzi et al., 1989), and dextromethorphan (Gorski et al., 1994). However, a few studies have shown marked differences in the inhibition kinetics between P450s 3A4 and 3A5. For example, significant differences have been seen for the mechanism-based inactivation of P450s 3A4 and 3A5 by mifepristone where P450 3A5 did not exhibit irreversible inhibition (Khan et al., 2002). Recently, verapamil was shown to be a selective inhibitor of P450 3A4 (Wang et al., 2005). In the search for additional specific probes that are capable of differentiating between these two major human 3A enzymes, two coumarin propargyl ether compounds were synthesized.

In this investigation, incubation of P450 3A4 with two structurally similar propargyl ethers, CPE and TFCPE, resulted in the loss of BFC *O*-debenzylation activity in a time- and concentration-dependent manner. The inactivation of P450 3A4 by CPE and TFCPE was characterized by K_I values of 112 and 14 μM, k_{inact} values of 0.05 and 0.04 min^{-1}, and half times of 13.9 and 16.5 min, respectively (Table 1). Because mechanism-based inactivation can be substrate-dependent and studies have shown that P450 3A4 can

accommodate more than one of the same or different substrate molecules in its active site (Korzekwa et al., 1998), we used testosterone as an additional substrate to measure the effect of the two propargyl ethers on the hydroxylation activity of P450 3A4. CPE and TFCPE both caused a loss of the 6-β testosterone hydroxylation activity of P450 3A4 in a time-, concentration-, and NADPH-dependent manner and demonstrated pseudo-first order kinetics. The inactivation's were characterized by a K_I of 25 μM, a k_{inact} of 0.014 min^{-1}, and a $t_{1/2}$ of 50 min for CPE and a K_I of 17 μM, a k_{inact} of 0.04 min^{-1}, and a $t_{1/2}$ of 17 min for TFCPE. This type of substrate-dependent effect on P450 3A4 inhibition has been shown before (Kenworthy et al., 1999). Wang et al have also shown that 3A4 inhibition as measured by different probes such as testosterone, nifedipine and midazolam is substrate-dependent (Wang et al., 2000). Thus differences in the kinetic parameters seen with CPE could be substrate-dependent. Interestingly, neither CPE nor TFCPE showed any effect on the BFC *O*-debenzylation activity of P450 3A5. Because P450 3A5 does not efficiently catalyze the hydroxylation of testosterone (Wrighton et al., 1990) or progesterone (Aoyama et al., 1989), we did not investigate the effects of CPE or TFCPE on steroid metabolism by 3A5. Although neither CPE nor TFCPE compounds resulted in the loss of BFC activity, they both were *O*-dealkylated to form 7-hydroxycoumarin by 3A4 and 3A5, as detected by HPLC with fluorescence detection (Table 3).

These results suggest that metabolism of both of the propargyl ethers by P450 3A5 occurs but may not produce the reactive intermediate necessary to bring about a loss in function of this enzyme. Several reports have shown differences in the inactivation or metabolism of various substrates by P450 3A4 and 3A5. Similar findings have been identified where P450 3A5 has been shown to oxidize vincristine and tacrolimus more efficiently than

3A4 (Dennison et al., 2006) and differential inactivation of 3A4 and 3A5 by raloxifene has been observed (Baer et al., 2007). Both compounds also inactivated rat P450 2B1 in the reconstituted system in a time-, concentration-, and NADPH-dependent manner (data not shown). Incubation of these compounds at concentrations up to 100 μM in the presence of NADPH showed no inactivation of human P450 2C9 and 2E1. When incubated with human liver microsomes, neither CPE nor TFCPE led to any inactivation of the P450s as measured by the BFC assay (data not shown). This could be because other P450s present in the microsomes may play predominant roles in the metabolism of these compounds so that relatively little metabolism occurs by 3A4 or 3A5 and therefore the amount of inactivation is negligible. We have seen similar results with some other mechanism-based inactivators we have studied.

Spectral analysis showed some loss of heme upon inactivation suggesting that the inactivation of P450 3A4 could be due to both heme and apoprotein modifications (Table 2). A small peak corresponding to heme adduct was detected by HPLC when the sample was monitored at 405 nm. The diode array spectrum of the peak was similar to the native heme spectrum (data not shown). However, LC-MS analysis of the TFCPE modified P450 3A4 did not reveal a heme adduct suggesting that the modified heme may not have been stable under the LC-MS conditions used. We have not yet been able to identify the adducts formed by CPE- or TFCPE with P450 primarily because modified P450 3A4 has a tendency to aggregate and is difficult to analyze the inactivated protein using whole protein mass spectrometry. For this reason, we chose to determine the structures of the CPE- or TFCPE- reactive intermediates using GSH. GSH adducts of CPE and TFCPE were observed by LC-MS after incubation with P450 3A4 indicating that reactive

electrophilic intermediates were generated during the metabolism and inactivation. Figures 4 and 5 show the GSH adducts of the propargyl ether compounds and their fragmentation patterns. As shown in these figures, the typical ions that are characteristic of GSH adducts were identified. However, fragmentation of the coumarin compounds themselves was not observed. As shown in Figs 4 and 5, the masses and MS/MS ion fragmentation patterns appear to be consistent with adduction of GSH, although it is not clear whether adduct formation occurs at the internal or the external carbon of the ethynyl moiety. Similar retention times were observed using a fluorescence detector that confirmed the presence of a fluorescent GSH adduct. The metabolism of TFCPE by P450 3A4 in a reconstituted system was investigated using LC-APCI-UV analysis. Following a 60 min incubation with P450 3A4, one NADPH-dependent peak was observed using UV detection at 319 nm with a retention time of 20.34 min. The retention time of the parent compound TFCPE was 22.78 min. The metabolite peak was observed only in the samples that were incubated with P450 3A4 in presence of TFCPE. No similar peak or any other metabolite peak was observed under these conditions. The proposed structures of the observed metabolite and the parent are depicted in Figures 6 and 7.

Using homology modeling, Lewis et al. (2006) have shown that metabolism of coumarin by several P450s can been rationalized in terms of likely interactions between coumarin and the active sites of the enzymes. They have shown that a combination of hydrogen bonding and π-π stacking with key amino acids within the heme environment may be responsible for positioning the coumarin substrate for metabolism. In comparing the residues that are in alignment between the SRS regions based on the P450 2C5 model, it has been suggested that phenylalanine at position 205 (in SRS2) may be associated with

the coumarin aromatic ring. Consequently, π-π stacking may occur between coumarin and the phenylalanine 205 residue. In addition, they suggest that at least one hydrogen bond forming amino-acid should interact with the coumarin molecule to facilitate the proper orientation in the active site and determine the site of metabolism. Although relatively closely related with respect to sequence, P450s 3A4 and 3A5 differ in 78 out of a total of 503 amino acids. 17 of these variations lie within the putative SRS domains and include the one at position 205. Thus, this active site difference could affect the binding of some substrates by these two enzymes and thus account for the different catalytic outcomes that were observed when P450s 3A4 and 3A5 metabolize the same propargyl coumarin compounds.

In conclusion, the synthesis of CPE and TFCPE, that combine the structure of a known substrate of the 3A P450s with a functional group that can be metabolized by these enzymes to a reactive intermediate has provided us with two inhibitors which are selective for P450 3A4 but do not affect the activity of P450 3A5. The placement of the propargyl groups on the known P450 substrate, coumarin, to yield compounds that inactivate P450 3A4 but fail to inactivate P450 3A5 supports the utility of coumarin propargyl ethers as useful structural probes in differentiating these enzymes *in vitro*.

Acknowledgements.

The authors would like to thank Hsia-Lien Lin for the purification of reductase and cytochrome b_5 and Dr. Haoming Zhang on the helpful discussion on the GSH adducts and Kien Anh Nguyen in synthesizing the compounds.

Reference List

Aoyama T, Yamano S, Waxman DJ, Lapenson DP, Meyer UA, Fischer V, Tyndale R, Inaba T, Kalow W, Gelboin HV, and . (1989) Cytochrome P-450 hPCN3, a novel cytochrome P-450 IIIA gene product that is differentially expressed in adult human liver. cDNA and deduced amino acid sequence and distinct specificities of cDNA-expressed hPCN1 and hPCN3 for the metabolism of steroid hormones and cyclosporine. *J.Biol.Chem.* **264**:10388-10395.

Baer BR, Wienkers LC, and Rock DA (2007a) Time-dependent inactivation of P450 3A4 by raloxifene: identification of Cys239 as the site of apoprotein alkylation. *Chem Res.Toxicol.* **20**:954-964.

Bargetzi MJ, Aoyama T, Gonzalez FJ, and Meyer UA (1989) Lidocaine metabolism in human liver microsomes by cytochrome P450IIIA4. *Clin Pharmacol.Ther.* **46**:521-527.

Blobaum AL, Kent UM, Alworth WL, and Hollenberg PF (2002) Mechanism-based inactivation of cytochromes P450 2E1 and 2E1 T303A by tert-butyl acetylenes: characterization of reactive intermediate adducts to the heme and apoprotein. *Chem.Res.Toxicol.* **15**:1561-1571.

Born SL, Fix AS, Caudill D, and Lehman-McKeeman LD (1998) Selective Clara cell injury in mouse lung following acute administration of coumarin. *Toxicol.Appl.Pharmacol.* **151**:45-56.

Buters JT, Schiller CD, and Chou RC (1993) A highly sensitive tool for the assay of cytochrome P450 enzyme activity in rat, dog and man. Direct fluorescence monitoring of the deethylation of 7-ethoxy-4-trifluoromethylcoumarin. *Biochem.Pharmacol.* **46**:1577-1584.

Cho US, Park EY, Dong MS, Park BS, Kim K, and Kim KH (2003) Tight-binding inhibition by alpha-naphthoflavone of human cytochrome P450 1A2. *Biochim.Biophys.Acta* **1648**:195-202.

Dennison JB, Kulanthaivel P, Barbuch RJ, Renbarger JL, Ehlhardt WJ, and Hall SD (2006a) Selective metabolism of vincristine in vitro by CYP3A5. *Drug Metab Dispos.* **34**:1317-1327.

Evans WE and Relling MV (1999) Pharmacogenomics: translating functional genomics into rational therapeutics. *Science* **286**:487-491.

Gibbs MA, Thummel KE, Shen DD, and Kunze KL (1999) Inhibition of cytochrome P-450 3A (CYP3A) in human intestinal and liver microsomes: comparison of Ki values and impact of CYP3A5 expression. *Drug Metab Dispos.* **27**:180-187.

Gillam EM, Baba T, Kim BR, Ohmori S, and Guengerich FP (1993) Expression of modified human cytochrome P450 3A4 in Escherichia coli and purification and reconstitution of the enzyme. *Arch.Biochem.Biophys.* **305**:123-131.

Gillam EM, Guo Z, Ueng YF, Yamazaki H, Cock I, Reilly PE, Hooper WD, and Guengerich FP (1995b) Expression of cytochrome P450 3A5 in Escherichia coli: effects of 5' modification, purification, spectral characterization, reconstitution conditions, and catalytic activities. *Arch.Biochem.Biophys.* **317**:374-384.

Gorski JC, Hall SD, Jones DR, VandenBranden M, and Wrighton SA (1994) Regioselective biotransformation of midazolam by members of the human cytochrome P450 3A (CYP3A) subfamily. *Biochem.Pharmacol.* **47**:1643-1653.

Hanna IH, Teiber JF, Kokones KL, and Hollenberg PF (1998) Role of the alanine at position 363 of cytochrome P450 2B2 in influencing the N. *Arch.Biochem.Biophys.* **350**:324-332.

Kamdem LK, Streit F, Zanger UM, Brockmoller J, Oellerich M, Armstrong VW, and Wojnowski L (2005) Contribution of CYP3A5 to the in vitro hepatic clearance of tacrolimus. *Clin.Chem* **51**:1374-1381.

Khan KK, He YQ, Correia MA, and Halpert JR (2002) Differential oxidation of mifepristone by cytochromes P450 3A4 and 3A5: selective inactivation of P450 3A4. *Drug Metab Dispos.* **30**:985-990.

Korzekwa KR, Krishnamachary N, Shou M, Ogai A, Parise RA, Rettie AE, Gonzalez FJ, and Tracy TS (1998) Evaluation of atypical cytochrome P450 kinetics with two-substrate models: evidence that multiple substrates can simultaneously bind to cytochrome P450 active sites. *Biochemistry* **37**:4137-4147.

Kuehl P, Zhang J, Lin Y, Lamba J, Assem M, Schuetz J, Watkins PB, Daly A, Wrighton SA, Hall SD, Maurel P, Relling M, Brimer C, Yasuda K, Venkataramanan R, Strom S, Thummel K, Boguski MS, and Schuetz E (2001a) Sequence diversity in CYP3A promoters and characterization of the genetic basis of polymorphic CYP3A5 expression. *Nat.Genet.* **27**:383-391.

Lake B.G. (1999) Coumarin Metabolism, Toxicity and Carcinogenicity: Relevance for Human Risk Assessment. *Food and Chemical Toxicity* **37**:423-453.

Marshall ME, Butler K, Cantrell J, Wiseman C, and Mendelsohn L (1989) Treatment of advanced malignant melanoma with coumarin and cimetidine: a pilot study. *Cancer Chemother.Pharmacol.* **24**:65-66.

Ortiz de Montellano PR and Kunze KL (1980) Self-catalyzed inactivation of hepatic cytochrome P-450 by ethynyl substrates. *J.Biol.Chem.* **255**:5578-5585.

Roberts ES, Hopkins NE, Foroozesh M, Alworth WL, Halpert JR, and Hollenberg PF (1997) Inactivation of cytochrome P450s 2B1, 2B4, 2B6, and 2B11 by arylalkynes. *Drug Metab Dispos.* **25**:1242-1248.

Roberts ES, Hopkins NE, Zaluzec EJ, Gage DA, Alworth WL, and Hollenberg PF (1994) Identification of active-site peptides from 3H-labeled 2-ethynylnaphthalene-inactivated P450 2B1 and 2B4 using amino acid sequencing and mass spectrometry. *Biochemistry* **33**:3766-3771.

Shimada T, Yamazaki H, Foroozesh M, Hopkins NE, Alworth WL, and Guengerich FP (1998) Selectivity of polycyclic inhibitors for human cytochrome P450s 1A1, 1A2, and 1B1. *Chem Res.Toxicol.* **11**:1048-1056.

Soine T.O (1964) Naturally occuring coumarins and related physiological activities. *Journal of Pharmaceutical Sciences* **53**:231-264.

Strobel SM, Szklarz GD, He Y, Foroozesh M, Alworth WL, Roberts ES, Hollenberg PF, and Halpert JR (1999) Identification of selective mechanism-based inactivators of cytochromes P-450 2B4 and 2B5, and determination of the molecular basis for differential susceptibility. *J.Pharmacol.Exp.Ther.* **290**:445-451.

Teiber JF and Hollenberg PF (2000) Identification of the human liver microsomal cytochrome P450s involved in the metabolism of N-nitrosodi-n-propylamine. *Carcinogenesis* **21**:1559-1566.

Von Weymarn LB, Sridar C, and Hollenberg PF (2004) Identification of amino acid residues involved in the inactivation of cytochrome P450 2B1 by two acetylenic compounds: the role of three residues in nonsubstrate recognition Sites. *J.Pharmacol.Exp.Ther.* **311**:71-79.

Wandel C, Bocker R, Bohrer H, Browne A, Rugheimer E, and Martin E (1994) Midazolam is metabolized by at least three different cytochrome P450 enzymes. *Br.J.Anaesth.* **73**:658-661.

Wang RW, Newton DJ, Liu N, Atkins WM, and Lu AY (2000) Human cytochrome P-450 3A4: in vitro drug-drug interaction patterns are substrate-dependent. *Drug Metab Dispos.* **28**:360-366.

Wang YH, Jones DR, and Hall SD (2005) Differential mechanism-based inhibition of CYP3A4 and CYP3A5 by verapamil. *Drug Metab Dispos.* **33**:664-671.

Wrighton SA, Brian WR, Sari MA, Iwasaki M, Guengerich FP, Raucy JL, Molowa DT, and VandenBranden M (1990) Studies on the expression and metabolic capabilities of human liver cytochrome P450IIIA5 (HLp3). *Mol.Pharmacol.* **38**:207-213.

Wrighton SA, Schuetz EG, Thummel KE, Shen DD, Korzekwa KR, and Watkins PB (2000) The human CYP3A subfamily: practical considerations. *Drug Metab Rev.* **32**:339-361.

Wrighton SA and Stevens JC (1992) The human hepatic cytochromes P450 involved in drug metabolism. *Crit Rev.Toxicol.* **22**:1-21.

Footnotes.

The study was supported in part by an MBRS/SCORE Grant (MF) from NIH NIGMS Institute (S06 GM 08008) and by National Institutes of Health Grant CA 16954 (PFH).

Figure Legends

Figure 1. Chemical structures of CPE and TFCPE

Figure 2. Time- and concentration-dependent inactivation of P450 3A4 by CPE. P450 3A4 was reconstituted with reductase and incubated with different concentrations of CPE as described in Materials and Methods. The concentrations of CPE that were used were **(◇) 0 μM; (■) 25 μM; (□), 50 μM; (▲) 100 μM; (Δ) 175 μM; (●) 250 μM; and (○)** 500 μM. The data represent the means and standard errors from 4 experiments. The inset shows a double reciprocal plot of the inverse of rates of inactivation versus the inverse of the CPE concentrations.

Figure 3. Time- and concentration-dependent inactivation of P450 3A4 by TFCPE. P450 3A4 was reconstituted with reductase and incubated with different concentrations of TFCPE as described in Materials and Methods. The concentrations of TFCPE that were used were (■) 0 μM; (□), 5 μM; (▲) 10 μM; (Δ) 25μM; (●) 50 μM; and (○) 100 μM. The data represent the means and standard errors from 4 experiments. The inset shows a double reciprocal plot of the inverse of rates of inactivation versus the inverse of the TFCPE concentrations.

Figure 4. Mass spectral analysis of the adduct of CPE with glutathione. P450 3A4 was reconstituted with reductase and lipid, incubated with CPE in the presence of GSH, and the samples were analyzed as described in the Materials and Methods. (A) Total ion chromatogram showing a primary peak eluting at 22.2 min. (B) monitoring of the column effluent fluorometrically shows elution of the fluorescent GSH adduct at 22.2 min (C) mass spectrum of the peak eluting at 11.8 with an (M+) ion at 523.9 (D) MS/MS of the

523.9 ion, (E) proposed structure of the CPE-GS adduct showing the primary fragmentations.

Figure 5. Mass spectral analysis of the adduct of TFCPE with glutathione. P450 3A4 was reconstituted with reductase and lipid, incubated with TFCPE in the presence of GSH, and samples were analyzed as described in the Materials and Methods. (A) Total ion chromatogram showing a primary peak eluting at 31.3 min. (B) monitoring of the column effluent fluorometrically shows elution of the fluorescent GSH adduct at 31.3 min (C) mass spectrum of the peak eluting at 31.3 min with an (M+) ion of 591.9 (D) MS/MS of the 591.9 ion, (E) proposed structure of the TFCPE-GS adduct showing the primary fragmentations.

Figure 6. LC-APCI-MS/MS analysis of TFCPE. P450 3A4 was reconstituted with reductase in the presence of TFCPE as described in the Materials and Methods. The reaction mixture was incubated at 37°C for 60 min and the metabolite(s) were extracted with ethyl acetate. The samples were then analyzed by LC-APCI-MS with UV monitoring at 319 nm. Panel A shows the UV of the parent and the metabolite peak and the inset shows the MS spectrum of the parent peak eluting at 22.78 min. Panel B shows the MS/MS analysis of the parent compound. Panel C shows the proposed fragmentation pattern of the parent compound leading to the peaks at m/z 240.9 and 212.9.

Figure 7. LC-APCI-MS/MS analysis of the metabolites of TFCPE formed by P450 3A4. The incubation conditions and analysis procedures are as described in Materials and Methods. Panel 7A shows the mass spectrum of the metabolite eluting at 20.34 min. Panels B and D show the MS/MS analyses of the 271 and 231 peaks respectively. Panels

C and E show the proposed fragmentation patterns for the peaks with m/z values of 271 and 231, respectively.

Table 1. Kinetic constants for the inactivation of P450 3A4 by CPE and TFCPE.

Substrate	**Inactivator**	K_I **(μM)**	K_{inact} **(min^{-1})**	$t_{1/2}$ **(min)**
BFC	**CPE**	112	0.05	13.9
	TFCPE	14	0.04	16.5
Testosterone	**CPE**	25	0.014	50
	TFCPE	17	0.04	17

Inactivation of the BFC O-debenzylation activity or testosterone β-hydroxylation activity of P450 3A4 was measured by incubating P450 3A4 with increasing concentrations of CPE or TFCPE. Aliquots of the sample were removed at different time points and assayed for residual activity as shown in Figs 2 and 3 for BFC. The kinetic constants were derived from the double reciprocal plots of the rates of inactivation as a function of inactivator concentration. The data shows the averages from three different experiments.

Table 2. Effect of CPE and TFCPE on the P450 3A4 BFC *O*-debenzylation activity, reduced CO spectrum, and residual heme as measured by HPLC.

P450 3A4	% Activity Remaining		% P450 Remaining by reduced-CO spectrum		Residual Heme by HPLC
	0 min	20 min	0 min	20 min	
-CPE, -NADPH	100	89 ± 2	100	92 ± 3	100
+CPE, -NADPH	86 ± 5	79 ± 3	69 ± 7	67 ± 2	100 ± 9
+CPE, +NADPH	85 ± 4	50 ± 9	69 ± 5	67 ± 4	70 ± 11
-TFCPE, -NADPH	100	89 ± 2	100	92 ± 1	100
+TFCPE, -NADPH	88 ± 3	79 ± 7	75 ± 4	62 ± 2	100 ± 4
+TFCPE, +NADPH	82 ± 5	25 ± 3	75 ± 6	43 ± 4	61 ± 2

Assay conditions are described under Materials and Methods. Activity remaining was determined using 50 μM concentration of CPE or 12 μM of TFCPE with an incubation time of 20 min. The amount of P450 remaining was measured using reduced-CO spectrum. The amount of residual heme by HPLC was calculated from the area under the heme peak as determined by absorbance at 405 nm. The area for the control sample was set to 100 %. The data represents the mean and standard deviation from 4 different experiments.

DMD Fast Forward. Published on July 24, 2008 as DOI: 10.1124/dmd.108.021493
This article has not been copyedited and formatted. The final version may differ from this version.

Table 3. Formation of 7-Hydroxycoumarin by P450s 3A4 and 3A5.

P450	Formation of 7-OH coumarin (pmol/pmol P450/min)	
3A4	CPE	48.1 ± 5
	TFCPE	97.2 ± 1
3A5	CPE	85.5 ± 7
	TFCPE	78.8 ± 11

The P450s were reconstituted in the presence of CPE or TFCPE as indicated in Materials and Methods. The formation of 7-hydroxycoumarin was measured by HPLC analysis with fluorescence detection. The data points represent the mean and average from 3 different experiments.

Figure 1

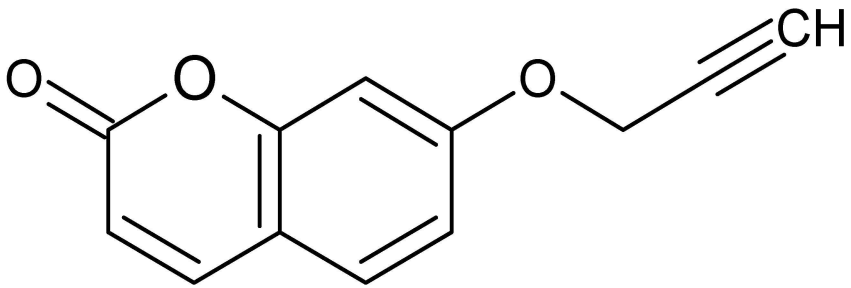

7-(coumarin) propargyl ether (CPE)
Mol wt : 200.2 g/mol

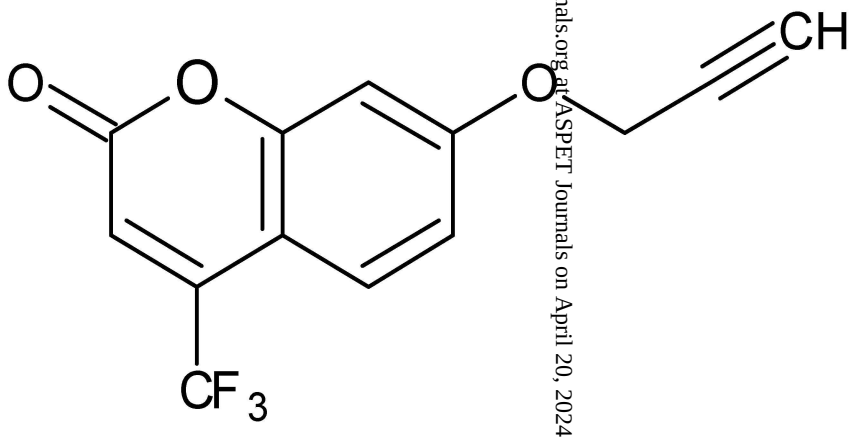

7-(4-trifluoromethyl) coumarin
Propargyl ether (TFCPE)
Mol Wt : 268.2 g/mol

Figure 2

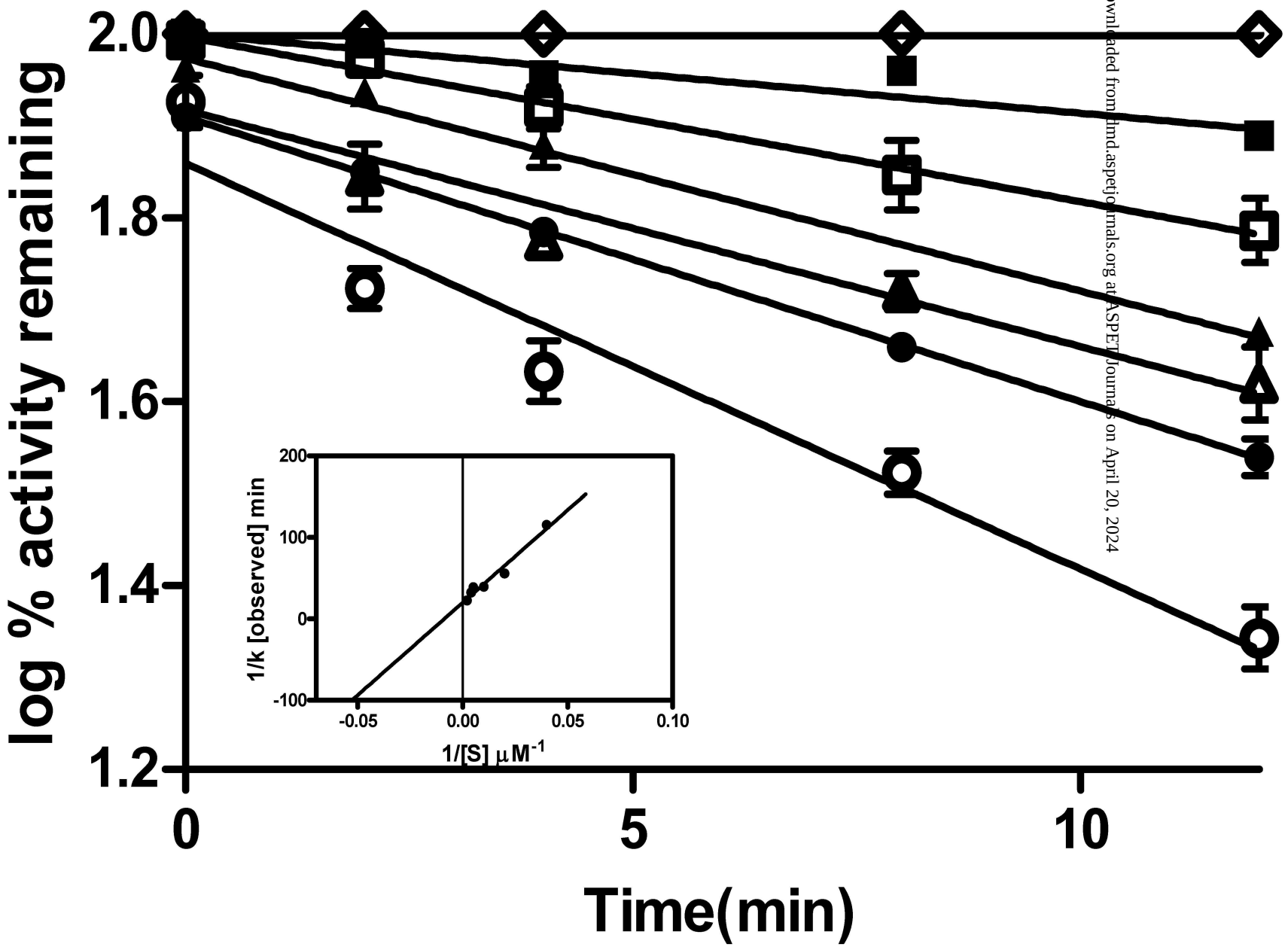

Figure 3

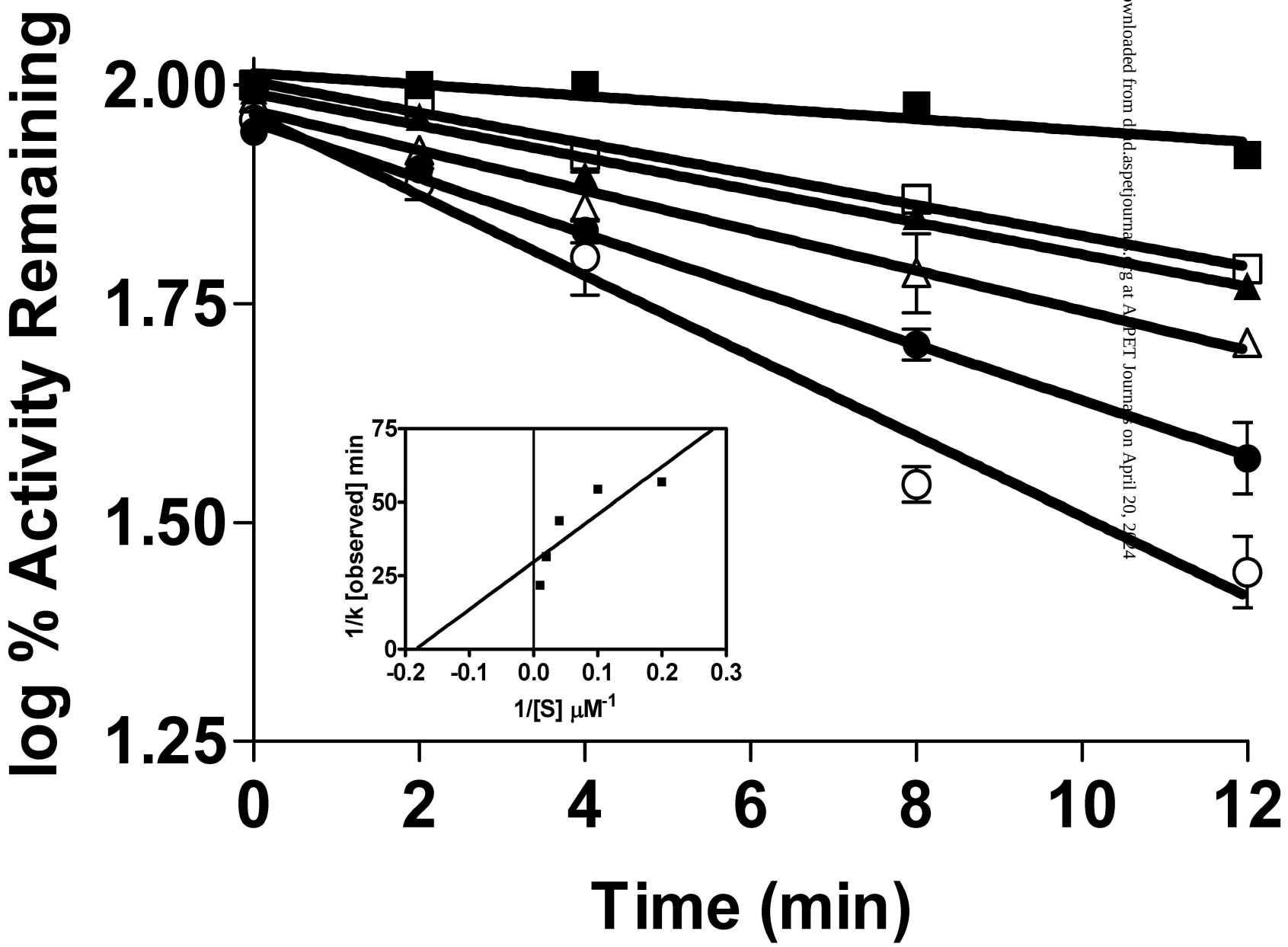

Figure 4

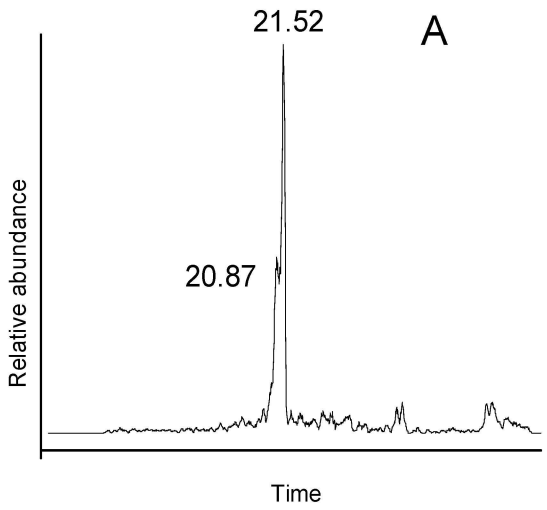

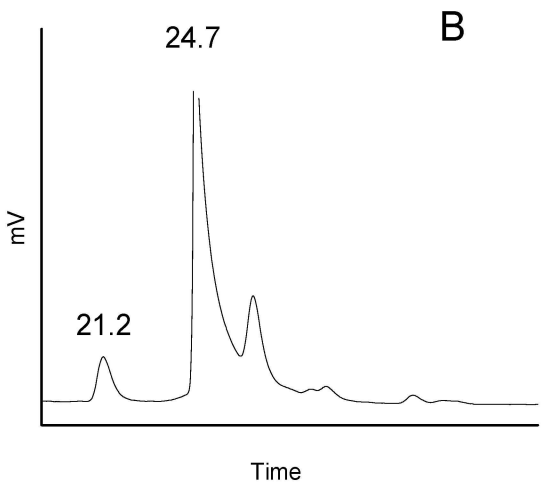

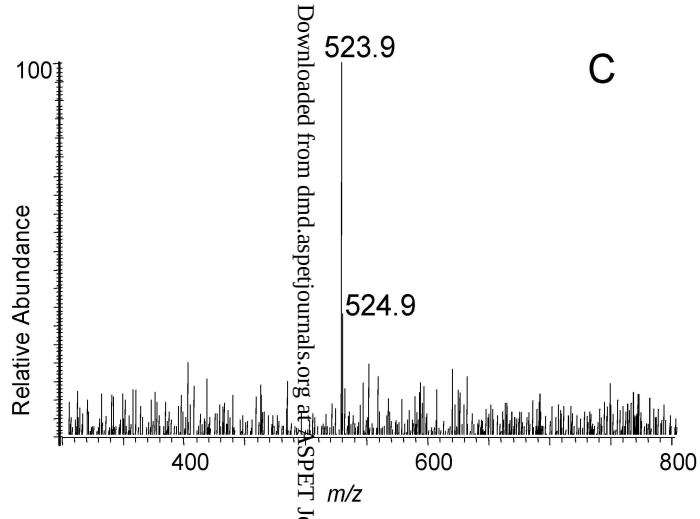

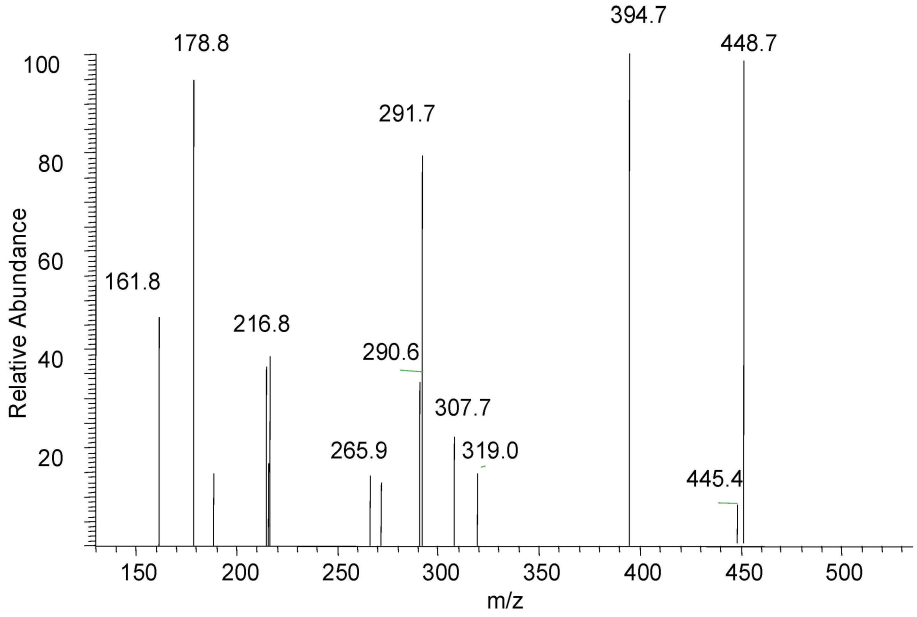

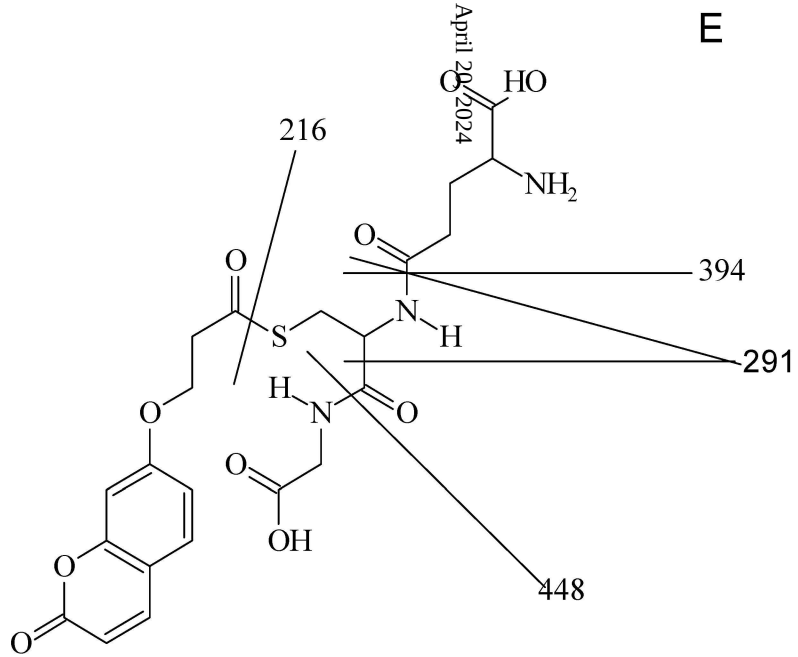

Figure 5

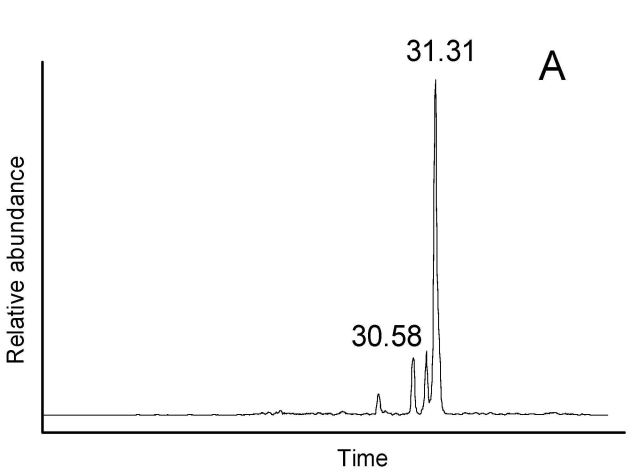

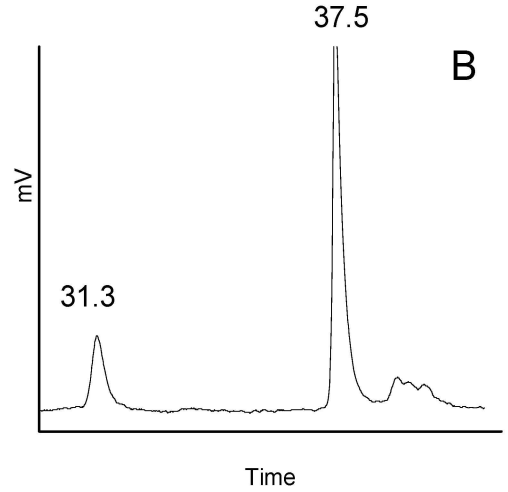

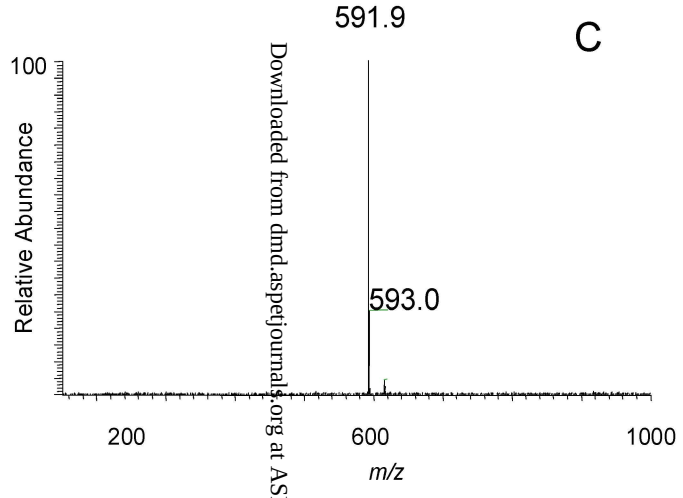

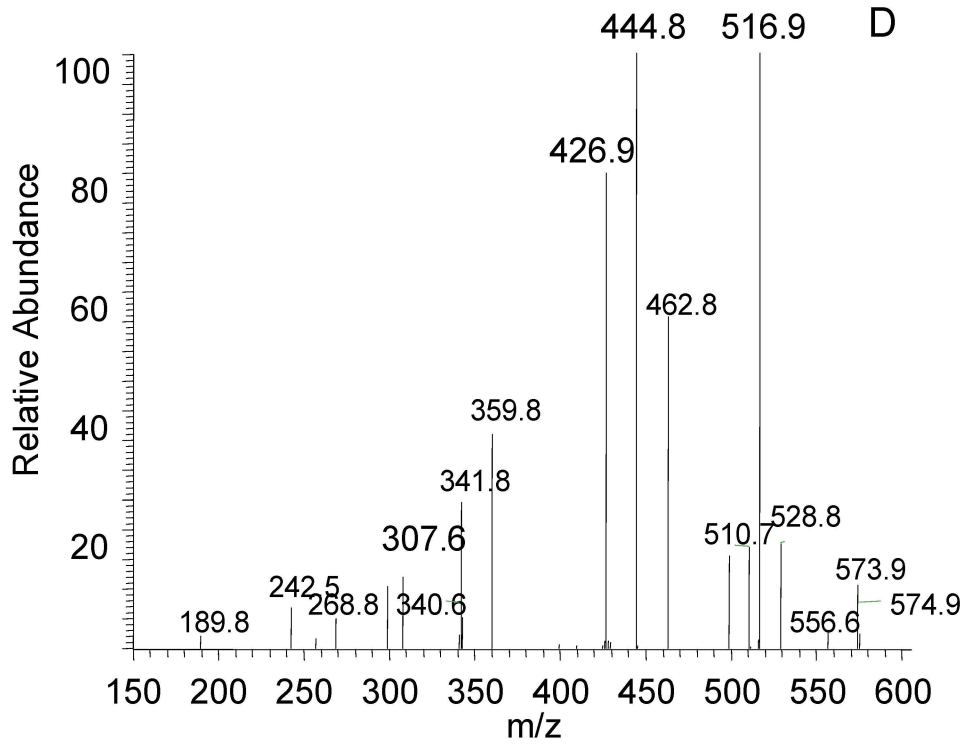

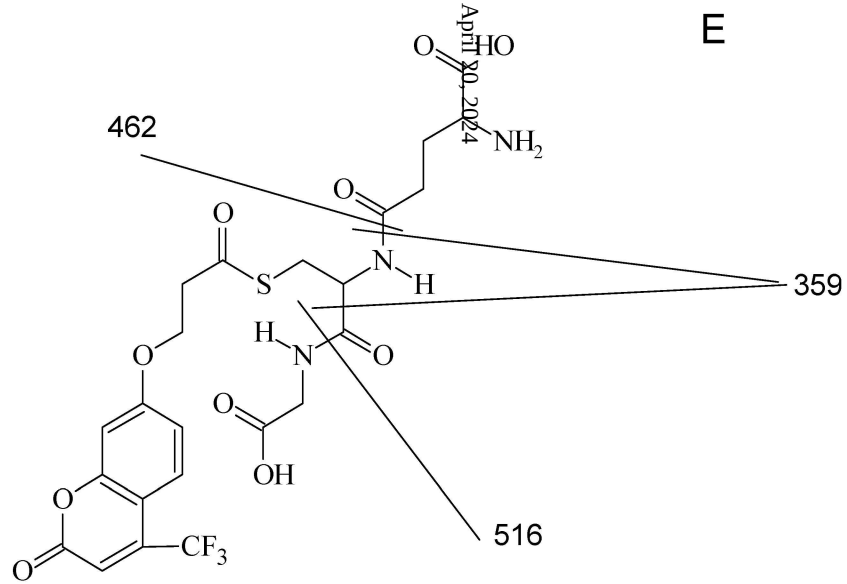

Figure 6

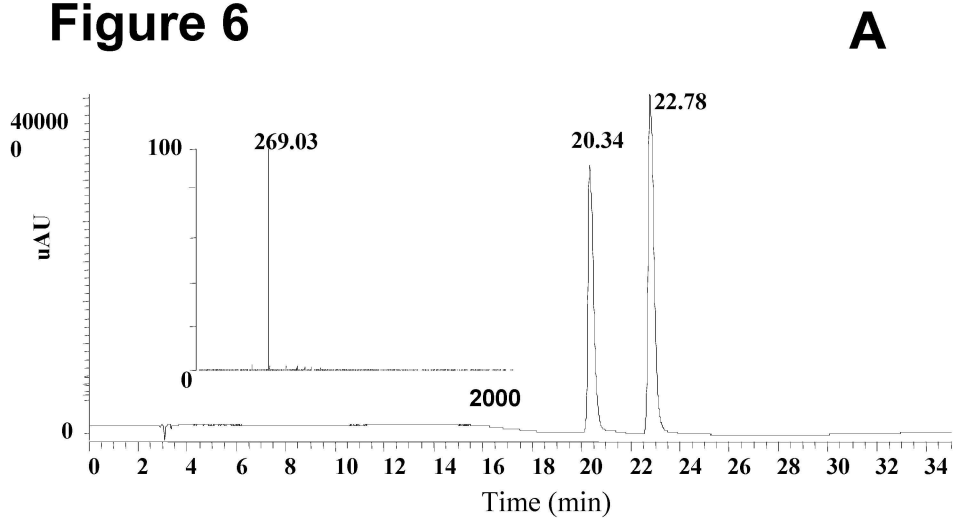

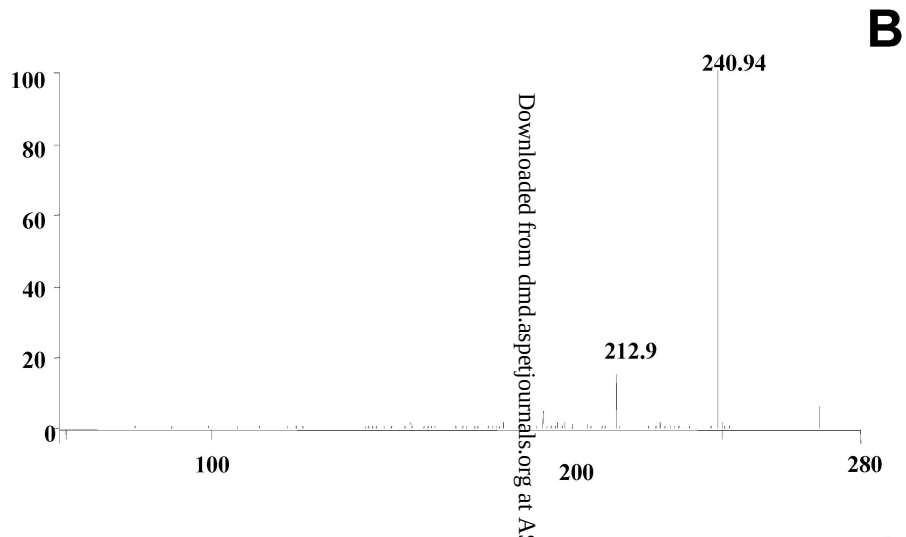

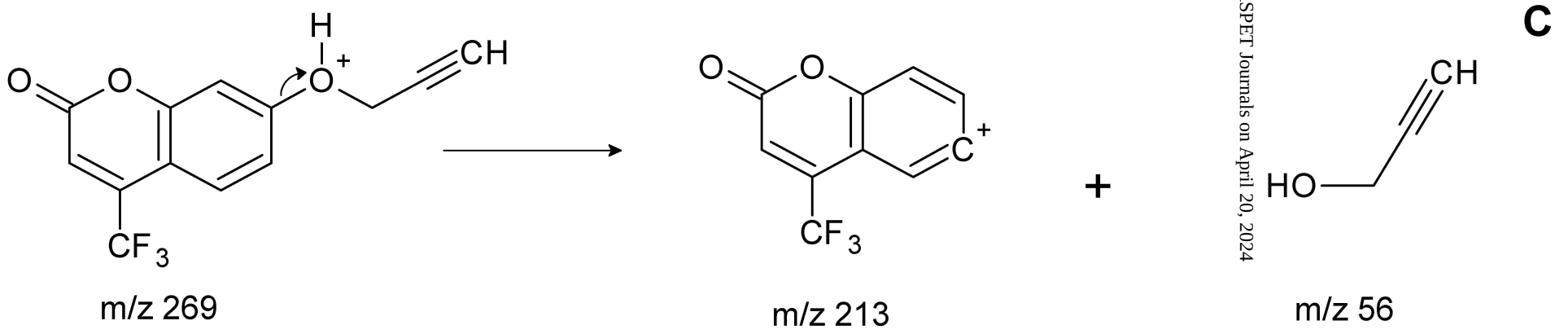

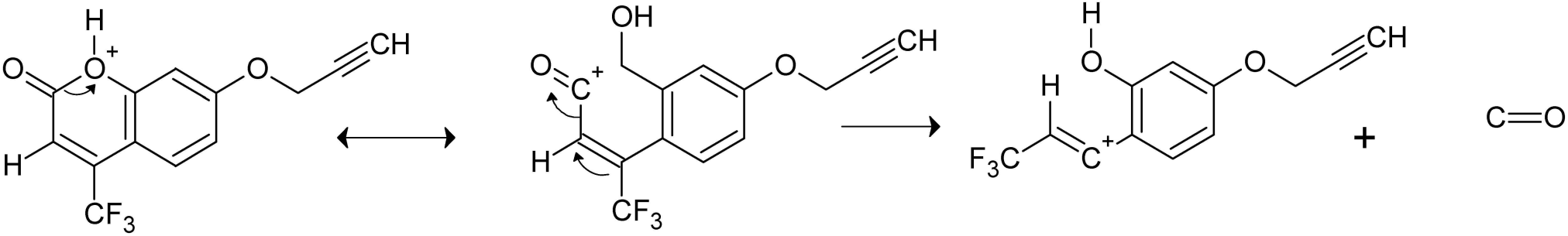

Figure 7

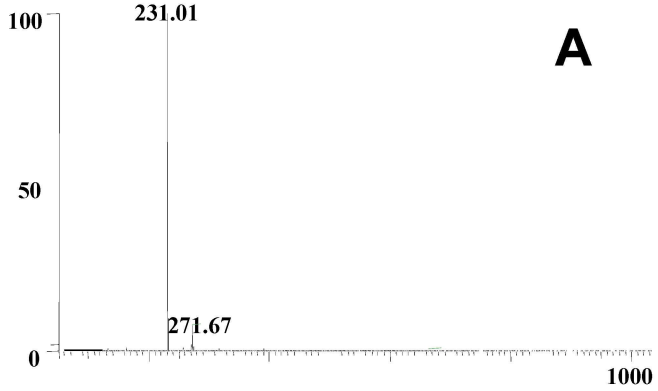

A

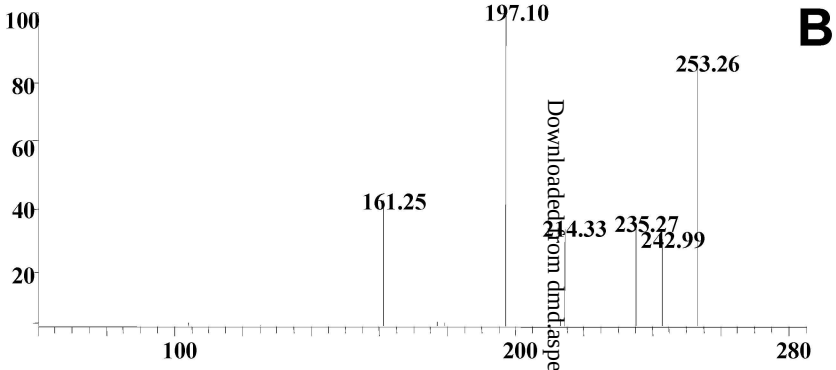

B

C

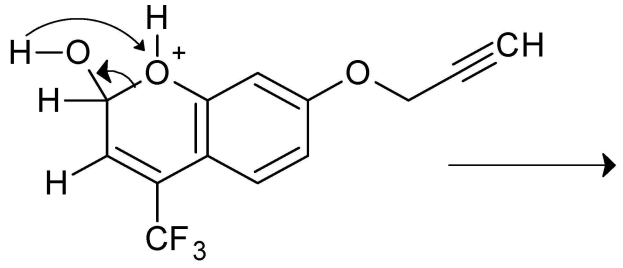

m/z 271

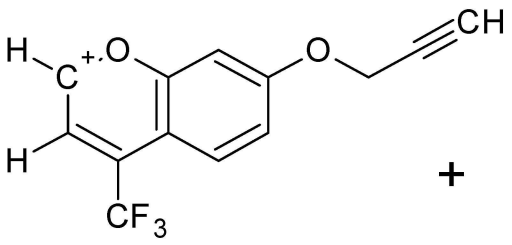

m/z 253

+ H_2O

18

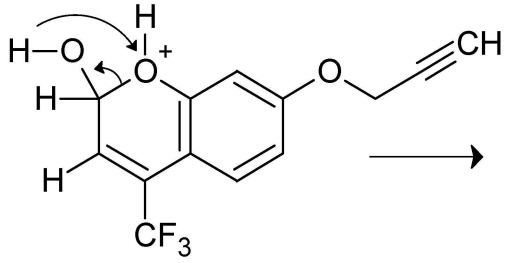

m/z 271

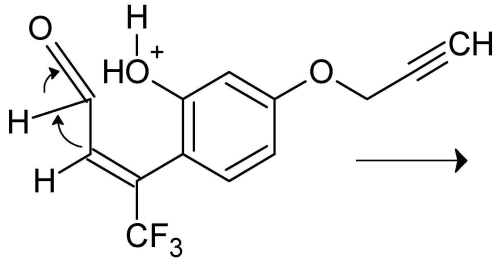

m/z 271

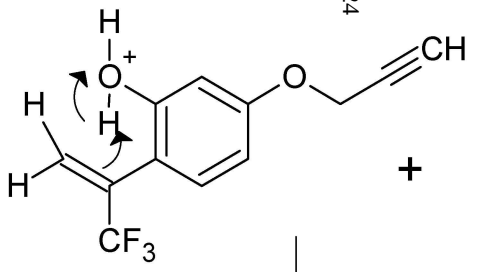

+ CO

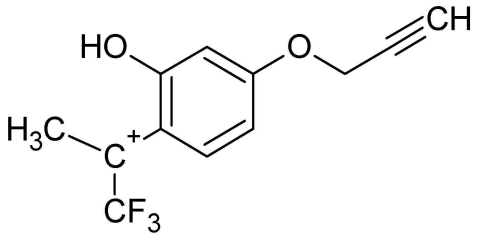

m/z 243

Figure 7

D

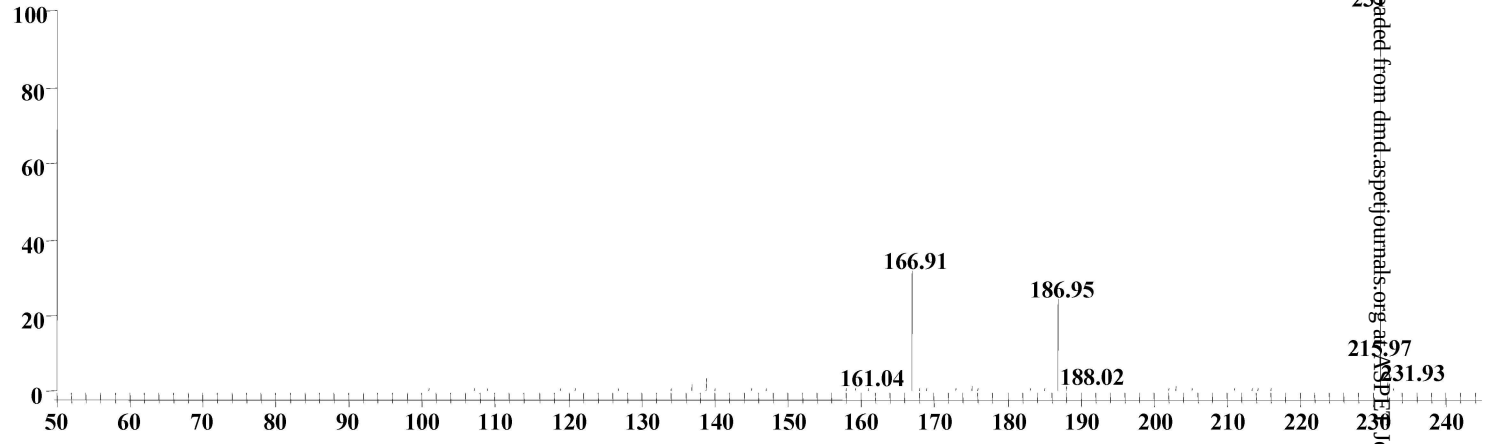

E

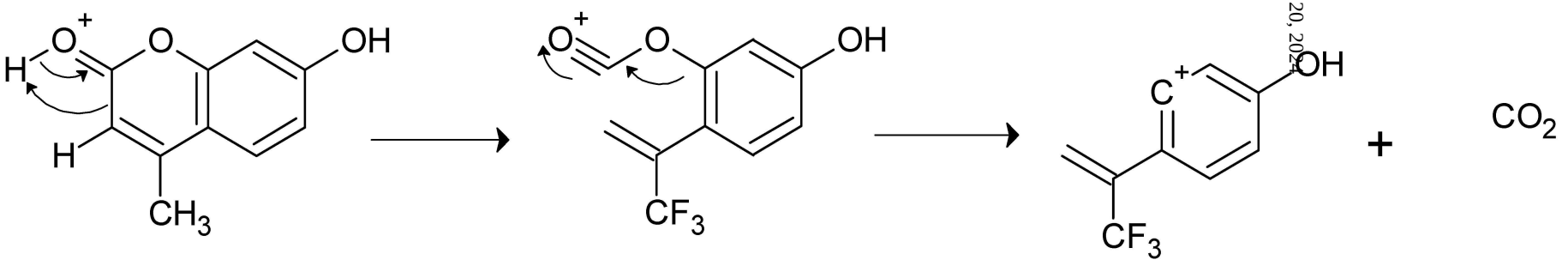

m/z 231 m/z 231 m/z 187 44